

Short Note

# 3-(3-Hydroxypropyl)-2,6-dioxo-1,2,3,6-tetrahydropyrimidine-4-carboxaldehyde Methyl Hemiacetal

Massimiliano Cordaro 

Dipartimento di Scienze Chimiche, Biologiche, Farmaceutiche e Ambientali, University of Messina, V.le F. Stagno D'Alcontres, 31, 98166 Messina, Italy; mcordaro@unime.it

**Abstract:** The synthesis of 3-(3-hydroxypropyl)-2,6-dioxo-1,2,3,6-tetrahydropyrimidine-4-carboxaldehyde as a stable methyl hemiacetal through a convenient 3-step procedure is reported. The molecule is multi-functional as it contains a formyl group, a hydroxyl group and the imide moiety. Each of these groups can play a role in specific transformations or uses.

**Keywords:** aldehydes; cyclization reaction; hemiacetal; low-cost procedures; solventless reactions; uracil derivatives

## 1. Introduction

Simple methods of preparation of aldehyde derivatives are of primary importance in organic synthesis. These precursors are basic and often unique starting points in the construction of more complex functional molecules for various applications [1–4]. In particular, the functionalization of important molecules such as nucleic acids with formyl groups can allow the derivatization for multiple application purposes [5–7]. Despite the fundamental role of nucleic acid derivatives in many biological processes, few examples of nucleic acids bearing aldehyde groups are reported so far [8,9]. No less important is the role that nucleic bases play thanks to their ability to interact with complementary functions through hydrogen bonds, as occurs in DNA. This feature makes them particularly useful for many applications in the field of supramolecular chemistry, molecular recognition and sensors [10–13].

## 2. Results and Discussion

In this work, the synthesis of 3-(3-hydroxypropyl)-2,6-dioxo-1,2,3,6-tetrahydropyrimidine-4-carboxaldehyde or 1-propanol-6-formyl-uracil **5**, through a convenient three-step procedure, is reported. The product is isolated by crystallization as a stable hemiacetal derivative from chromatographic solutions containing methanol. This efficient strategy involves the use of low-cost materials, a minimal amount of solvents and fast purification procedures. From ethyl acetoacetate **1** and methyl carbamate **2**, methyl oxazine **3** is isolated by crystallization from mother liquor in a 20% yield. Subsequently, the reaction of **3** with propanolamine in a sealed vial in solventless condition gives 1-propanol-6-methyl uracil **4** with 85% yield by crystallization, and finally, the oxidation with selenium dioxide allows to obtain uracil aldehyde **5** with 68 % yield, isolated after chromatographic column purification as hemiacetal derivative **5'** (Scheme 1).

Based on studies [9] and information reported in the literature [14,15], the sequence of the condensation reactions of ethyl acetoacetate **1** with methyl carbamate **2**, as reported in Scheme 2, could justify the low conversion yield of oxazine **3**. According to path (a), the nitrogen atom of the carbamate gives nucleophilic acyl substitution reaction, eliminates ethanol and an intermediate **6** is formed, which is in equilibrium with its tautomeric form **6'**, cyclizes and forms oxazine **3**. Product **3** precipitates as a white solid after cooling the mixture.



**Citation:** Cordaro, M.

3-(3-Hydroxypropyl)-2,6-dioxo-1,2,3,6-tetrahydropyrimidine-4-carboxaldehyde Methyl Hemiacetal.

*Molbank* **2021**, *2021*, M1272.

<https://doi.org/10.3390/M1272>

Academic Editor: Raffaella Mancuso

Received: 25 July 2021

Accepted: 17 August 2021

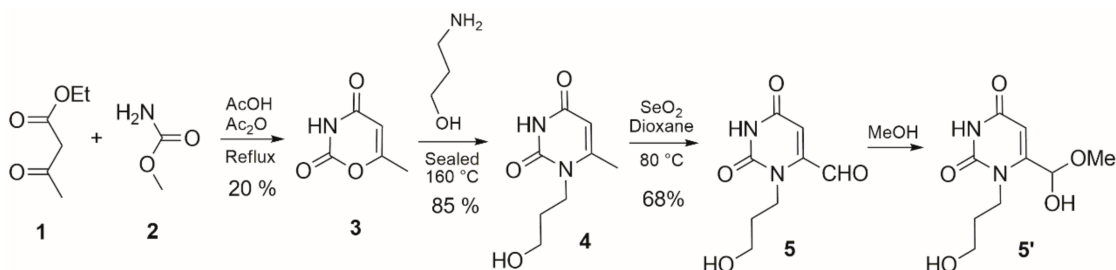
Published: 20 August 2021

**Publisher's Note:** MDPI stays neutral with regard to jurisdictional claims in published maps and institutional affiliations.

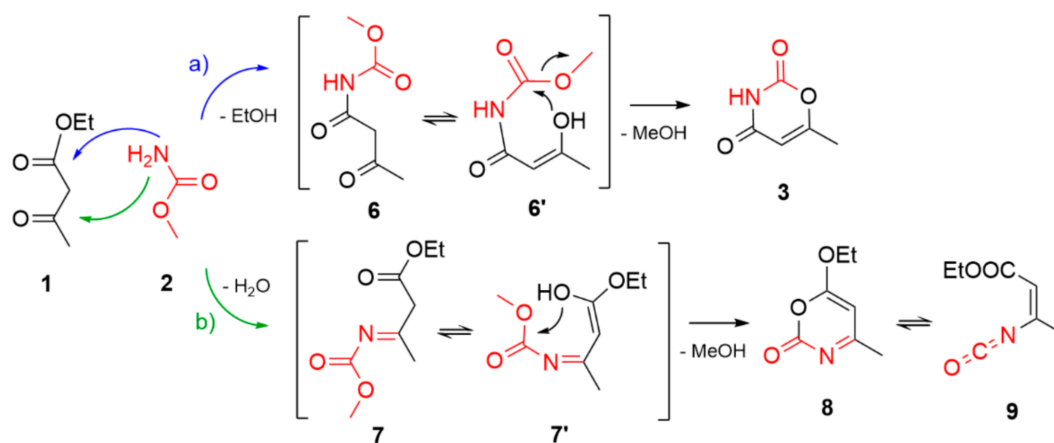


**Copyright:** © 2021 by the author. Licensee MDPI, Basel, Switzerland. This article is an open access article distributed under the terms and conditions of the Creative Commons Attribution (CC BY) license (<https://creativecommons.org/licenses/by/4.0/>).

The most probable course is the formation of imine intermediate **7** through path (b), which is in equilibrium with the tautomeric form **7'**, cyclizes and forms 2-ethoxy-4-methyl-1,3-oxazin-6-one **8**, which is in equilibrium with ethyl  $\beta$ -isocyanatocrotonate **9** in solution.

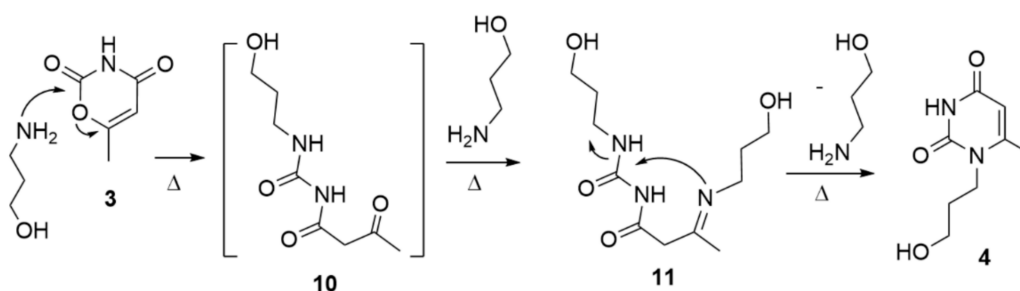


**Scheme 1.** The overall synthetic procedure of **5'**.



**Scheme 2.** The conceivable condensation reaction sequences of **1** and **2**.

1-(3-hydroxypropyl)-6-methylpyrimidine-2,4(1*H*,3*H*)-dione **4** is obtained through an elimination/cyclization mechanism of a stable open intermediate **11** formed by a double addition of amine, as shown in Scheme 3.



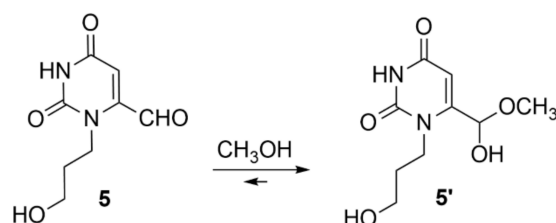
**Scheme 3.** The reaction sequence of the formation of **4**.

Finally, the methyl oxidation reaction is obtained with selenium dioxide at 80 °C in dioxane, as shown in Scheme 1. The uracil aldehyde hemiacetal **5'** was obtained with a yield of 68% as a white solid after chromatographic purification (10% methanol/dichloromethane) (Scheme 1). The formation of hemiacetal **5'** is evidenced by NMR analysis, and the <sup>1</sup>H-NMR spectrum shows a singlet at 4.37 ppm corresponding to three protons (see Supplementary Materials Figures S6 and S7).

Other eluent mixtures containing ethyl acetate or diethyl ether with chloroform or dichloromethane in various ratios were used, but no products were separated. Methanol in

the optimal ratio with dichloromethane was found to be fundamental for good separation. Eluents with a higher methanol/dichloromethane ratio do not allow good purification due to the elution of by-products.

The unexpected formation of a hemiacetal does not affect the reactivity of the aldehyde group as it is well known that the hemiacetals in solution are in equilibrium (Scheme 4).



**Scheme 4.** Hemiacetal equilibrium of 5 in methanol.

In this case, the formation of the hemiacetal favors the stability of the aldehyde as a solid product 5' and acts as a protecting group of the aldehyde which can be used without limitations for further manipulation. All compounds were characterized by IR, NMR and Mass analysis (see Supplementary Materials). These procedures offer an important starting point for designing a wide variety of formyl-uracil derivatives also on a large scale. Moreover, the hydroxyl group could be further modified, either by inserting functionalities through nucleophilic substitution, e.g., forming an ester, or through the formation of tosylates, substituting the group with other nucleophiles such as azides.

This work offers a new and convenient procedure for the synthesis of useful scaffolds, which can be employed as starting building blocks for the synthesis of many functional molecules as chromophores (e.g., porphyrins, BODIPY) aimed to obtain functional materials for a wide range of applications [16–18].

### 3. Materials and Methods

All NMR spectra were recorded with Varian 500 instrument (Agilent, Santa Clara, CA, USA). The IR spectra were carried out with a Bruker FT-IR ALPHA spectrometer (Bruker, Billerica, MA, USA), equipped with an ATR-platinum accessory. Melting points were determined using a BÜCHI B-545 apparatus (BÜCHI, Flawil, Switzerland).

6-Methyl-2H-1,3-oxazine-2,4(3H)-dione 3 was prepared according to the published method [9].

#### 3.1. 1-Propanol-6-methyl-uracil 4

Oxazine 3 (500 mg, 4 mmol) and propanolamine (580 mg, 8 mmol) are placed in a sealed vial, the mixture was stirred in an oil bath at 160 °C for a period of 6 h after the cap is removed, and the temperature was maintained for 30 min until the liquid has completely evaporated. After cooling, the mixture solidifies, and crystallization is carried out with methanol, a white solid precipitates, and after filtration, 616 mg of pure product 4 is isolated (yield 85%); m.p. 215–217 °C.

IR (neat): 3256, 3146, 3031, 2957, 2801, 1698, 1657, 1605, 1474, 1452, 1405, 1298, 1241, 1180, 1051, 888, 752, 674, 631 and 535  $\text{cm}^{-1}$ .

$^1\text{H-NMR}$  (500 MHz, ppm,  $\text{DMSO-}d_6$ ):  $\delta$  10.80 ( $s_{\text{broad}}$ , 1H, NH), 5.46 (s, 1H, CH-5), 4.57 ( $s_{\text{broad}}$ , 1H, OH) 3.76 (t, 2H,  $J = 7.5$  Hz,  $\text{CH}_2\text{-N}$ ), 3.42 (t, 2H,  $J = 6.1$  Hz,  $\text{CH}_2\text{-OH}$ ), 2.23 (s, 3H,  $\text{CH}_3$ ) and 1.68 (m, 2 H,  $\text{CH}_2\text{-CH}_2\text{-CH}_2$ ).

$^{13}\text{C-NMR}$  (125 MHz, ppm,  $\text{DMSO-}d_6$ ):  $\delta$  162.9 (C), 154.8 (C), 152.0 (C), 101.3 (CH), 58.5 ( $\text{CH}_2$ ), 41.6 ( $\text{CH}_2$ ), 31.8 ( $\text{CH}_2$ ) and 19.6 ( $\text{CH}_3$ ).

HRMS (MicrOTOF)  $m/z$ :  $[\text{M} + \text{H}]^+$  Calcd for  $\text{C}_8\text{H}_{12}\text{N}_2\text{O}_3$  185,092; Found 185.206.

### 3.2. 1-Propanol-6-formyl-uracil Methyl Hemiacetal 5'

1-propanol-6-methyl-uracil 4 (500 mg, 2.72 mmol) and Selenium dioxide (350 mg, 3 mmol) were dissolved in 10% acetic acid/dioxane solution (10 mL), and the reaction was stirred at 80 °C for a period of 24 h. The uracil derivative 5' was purified by column chromatography on silica and 10% methanol/dichloromethane as eluent; yield: 366 mg (68%); white solid; mp 195–196 °C.

IR (neat): 3262, 3157, 2963, 2813, 1705, 1650, 1395, 1346, 1255, 1238, 1169, 1061, 857, 761, 677, 619 and 533  $\text{cm}^{-1}$ .

$^1\text{H-NMR}$  (500 MHz, ppm,  $\text{DMSO-}d_6$ ):  $\delta$  11.16 ( $s_{\text{broad}}$ , 1H, NH), 5.61 (s, 1H, CH-5), 4.57 ( $s_{\text{broad}}$ , 1H, OH), 4.37 (s, 3H,  $\text{OCH}_3$ ), 3.70 (t, 2H,  $J = 7.4$  Hz,  $\text{CH}_2\text{-N}$ ), 3.41 ( $s_{\text{broad}}$ , 2H,  $\text{CH}_2\text{-OH}$ ) and 1.69 (m, 2H,  $\text{CH}_2\text{-CH}_2\text{-CH}_2$ ).

$^{13}\text{C-NMR}$  (125 MHz, ppm,  $\text{DMSO-}d_6$ ):  $\delta$  186.1 (CH), 163.4 (C), 161.6 (C), 157.8 (C), 152.0 (CH), 98.8 ( $\text{CH}_3$ ), 59.1 ( $\text{CH}_2$ ), 58.5 ( $\text{CH}_2$ ) and 31.9 ( $\text{CH}_2$ ).

HRMS (MicrOTOF)  $m/z$ :  $[\text{M} + \text{H}]^+$  Calcd for  $\text{C}_8\text{H}_{10}\text{N}_2\text{O}_4$  199,071; Found 199.103.

**Supplementary Materials:** The following are available online. Figure S1:  $^1\text{H-NMR}$  (500 Mhz,  $\text{DMSO-}d_6$ ) of 1-propanol-6-methyl-uracil 4. Figure S2:  $^{13}\text{C-NMR}$  (125 Mhz,  $\text{DMSO-}d_6$ ) of 1-propanol-6-methyl-uracil 4. Figure S3: MicrOTOF mass spectrum of 1-propanol-6-methyl-uracil 4. Figure S4: Expansion of mass spectrum of 1-propanol-6-methyl-uracil 4. Figure S5: FT-IR spectrum of neat 1-propanol-6-methyl-uracil 4. Figure S6:  $^1\text{H-NMR}$  (500 Mhz,  $\text{DMSO-}d_6$ ) of 1-propanol-6-formyl-uracil methyl hemiacetal 5'. Figure S7:  $^{13}\text{C-NMR}$  (125 Mhz,  $\text{DMSO-}d_6$ ) of 1-propanol-6-formyl-uracil methyl hemiacetal 5'. Figure S8: MicrOTOF mass spectrum of 1-propanol-6-formyl-uracil 5. Figure S9: Expansion of mass spectrum of 1-propanol-6-formyl-uracil 5. Figure S10: FT-IR spectrum of neat 1-propanol-6-formyl-uracil 5.

**Funding:** FFABR2017—Università di Messina.

**Data Availability Statement:** Not applicable.

**Conflicts of Interest:** The author declares no conflict of interest.

## References

1. Iha, R.K.; Wooley, K.L.; Nyström, A.; Burke, D.J.; Kade, M.J.; Hawker, C.J. Applications of Orthogonal “Click” Chemistries in the Synthesis of Functional Soft Materials. *Chem. Rev.* **2009**, *109*, 5620–5686. [[CrossRef](#)] [[PubMed](#)]
2. Tsogoeva, S.B. Recent advances in asymmetric organocatalytic 1,4-conjugate additions. *Eur. J. Org. Chem.* **2007**, *11*, 1701–1716. [[CrossRef](#)]
3. Singh, J.; Dutta, T.; Kim, K.-H.; Rawat, M.; Samddar, P.; Kumar, P. ‘Green’ synthesis of metals and their oxide nanoparticles: Applications for environmental remediation. *J. Nanobiotechnol.* **2018**, *16*, 84. [[CrossRef](#)] [[PubMed](#)]
4. LA Ganga, G.; Nardo, V.M.; Cordaro, M.; Natali, M.; Vitale, S.; Licciardello, A.; Nastasi, F.; Campagna, S. A functionalized, ethynyl-decorated, tetracobalt (iii) cubane molecular catalyst for photoinduced water oxidation. *Dalton Trans.* **2014**, *43*, 14926–14930. [[CrossRef](#)] [[PubMed](#)]
5. Jin, X.-Y.; Wang, R.-L.; Xie, L.-J.; Kong, D.-L.; Liu, L.; Cheng, L. A chemical photo-oxidation of 5-Methyl cytidines. *Adv. Synth. Catal.* **2019**, *361*, 4685–4690. [[CrossRef](#)]
6. Calabretta, A.; Wasserberg, D.; Posthuma-Trumpie, G.A.; Subramaniam, V.; Van Amerongen, A.; Corradini, R.; Tedeschi, T.; Sforza, S.; Reinhoudt, D.N.; Marchelli, R.; et al. Patterning of peptide nucleic acids using reactive microcontact printing. *Langmuir* **2011**, *27*, 1536–1542. [[CrossRef](#)] [[PubMed](#)]
7. Dohno, C.; Shibata, T.; Nakatani, K. Discrimination of N6-methyl adenine in a specific DNA sequence. *Chem. Commun.* **2010**, *46*, 5530–5532. [[CrossRef](#)] [[PubMed](#)]
8. Shi, X.; Barkigia, K.M.; Fajer, J.; Drain, C.M. Design and Synthesis of Porphyrins Bearing Rigid Hydrogen Bonding Motifs: Highly Versatile Building Blocks for Self-Assembly of Polymers and Discrete Arrays. *J. Org. Chem.* **2001**, *66*, 6513–6522. [[CrossRef](#)] [[PubMed](#)]
9. Trapani, M.; Elemans, H.; Castriciano, M.A.; Nicosia, A.; Mineo, P.G.; Cordaro, M. A convenient synthetic approach to obtain meso-Uracil-BODIPY. *Synlett* **2021**. [[CrossRef](#)]
10. Du, X.; Zhou, J.; Shi, J.; Xu, B. Supramolecular hydrogelators and hydrogels: From soft matter to molecular biomaterials. *Chem. Rev.* **2015**, *115*, 13165–13307. [[CrossRef](#)] [[PubMed](#)]
11. Rohs, R.; West, S.; Sosinsky, A.; Liu, P.; Mann, R.S.; Honig, B. The role of DNA shape in protein–DNA recognition. *Nat. Cell Biol.* **2009**, *461*, 1248–1253. [[CrossRef](#)] [[PubMed](#)]
12. Liu, J.; Cao, Z.; Lu, Y. Functional nucleic acid sensors. *Chem. Rev.* **2009**, *109*, 1948–1998. [[CrossRef](#)] [[PubMed](#)]

13. Scala, A.; Cordaro, M.; Mazzaglia, A.; Risitano, F.; Venuti, A.; Sciortino, M.T.; Grassi, G. Aldol-type compounds from water-soluble indole-3,4-diones: Synthesis, kinetics, and antiviral properties. *Mol. Divers.* **2013**, *17*, 479–488. [[CrossRef](#)]
14. Kricheldorf, H.R. Reversible Isomerization in  $\beta$ -Isocyanatocrotonic Esters. *Angew. Chem. Int. Ed.* **1972**, *11*, 128–129. [[CrossRef](#)]
15. Schmidt, R.R.; Schwille, D.; Wolf, H. 3-Aza-pyrylium-Salze, VI. Alkyliden-1.3-oxazine und Alkyliden-pyrimidine. *Eur. J. Inorg. Chem.* **1970**, *103*, 2760–2767. [[CrossRef](#)]
16. Fresch, E.; Peruffo, N.; Trapani, M.; Cordaro, M.; Bella, G.; Castriciano, M.A.; Collini, E. The effect of hydrogen bonds on the ultrafast relaxation dynamics of a BODIPY dimer. *J. Chem. Phys.* **2021**, *154*, 084201. [[CrossRef](#)]
17. Panniello, A.; Trapani, M.; Cordaro, M.; DiBenedetto, C.N.; Tommasi, R.; Ingrosso, C.; Fanizza, E.; Grisorio, R.; Collini, E.; Agostiano, A.; et al. High-Efficiency FRET Processes in BODIPY-Functionalized Quantum Dot Architectures. *Chem. Eur. J.* **2021**, *27*, 2371–2380. [[CrossRef](#)] [[PubMed](#)]
18. Cordaro, M.; Mineo, P.; Nastasi, F.; Magazzù, G. Facile synthesis of boronic acids on a BODIPY core with promising sensitivity towards polyols. *RSC Adv.* **2014**, *4*, 43931–43933. [[CrossRef](#)]